FULL-SCALE MOTIONS OF A LARGE HIGH-SPEED CATAMARAN: THE INFLUENCE OF WAVE ENVIRONMENT, SPEED AND RIDE CONTROL SYSTEM

(DOI No: 10.3940/rina.ijme.2012.a3.238)

G Jacobi[1] and **G Thomas**, Australian Maritime College, University of Tasmania, Australia
M R Davis and **D S Holloway**, University of Tasmania, Australia
G Davidson and **T Roberts**, Revolution Design Pty Ltd, Tasmania, Australia

SUMMARY

To assess the behaviour of large high-speed catamarans in severe seas, extensive full-scale trials were conducted by the U.S. Navy on an INCAT Tasmania built vessel in the North Sea and North Atlantic region. Systematic testing was done for different speeds, sea states and ride control settings at different headings. Collected data has been used to characterise the ship's motions and seakeeping performance with respect to wave environment, vessel speed and ride control system. Motion response amplitude operators were derived and compared with results from a two-dimensional Green function time-domain strip theory seakeeping prediction method. An increase of motion response with increasing vessel speed and a decrease with the vessel moving from head to beam seas was found. In higher sea states and headings ahead of beam seas an increasing influence of the centre bow on pitch motion damping was found. Significant motion RAO reduction was also found when the ride control system was active. Its effectiveness increased at higher speeds and contributed to heave and pitch motion RAO reduction. Predicted motion magnitudes with the time domain seakeeping code were consistent with the measured motion responses, but maximum heave was predicted at a rather higher frequency than was evident in the trials.

[1] Intern Research Student from University of Rostock, Germany

NOMENCLATURE

c	Source location (m)
f	Source function
Fr	Froude number
g	Acceleration due to gravity (m/s^2)
$H_{1/3}$	Significant wave height (m)
i	Number of collocation points
j	Number of panels
k	Wavenumber
L	Ship length (m)
LCG	Longitudinal centre of gravity (m)
n	Normal vector
U	Ship forward speed (m/s)
p	Pressure (N/m^2)
Q	Source strength
s	Panel surface
$S(\omega_e)$	Energy density spectrum (m^2/(rad/s))
W	Complex velocity (m/s)
x_{30}, x_{40}, x_{50}	Heave, roll and pitch motion (m)
z	Complex coordinate of collocation point (m)
β	Slope of source element (rad)
ζ_0	Wave elevation (m)
ρ	Density of water (kg/m^3)
φ	Velocity potential (m^2/s)
ψ	Stream function (m^2/s)
ω_e	Encounter frequency (rad/s)
ω_e*	Dimensionless encounter frequency

1. INTRODUCTION

The growing demand of both commercial and military high-speed ships in recent years has led to the development of large high-speed catamarans with a high deadweight to lightship ratio. To compete against other means of transportation there is a steady effort to obtain higher speeds and payloads. As a result the structural weight is minimised by optimising the vessel's structure to a critical level with lightweight materials. While growing in size to obtain higher deadweights the vessels have to operate not only at high speeds but also in more severe conditions and higher sea states to guarantee reliable operation in any condition, particularly for military operations. Besides affecting the demands of adequate structural strength, the trend to lighter and faster ships also influences the motion response to encountered waves. The high Froude number and slender lightweight demihulls lead to higher vertical displacements with associated high heave and pitch motions within a certain range of encounter frequency. Response amplitude operators (RAOs) describing the ratio of vessel motion to the sea surface motion will thus have maxima significantly exceeding unity [1]. This strong motion response can promote motion sickness and passenger discomfort. Though absolute roll motions are found to be smaller for twin hull geometries they can exhibit high lateral accelerations due to the wide spacing of the demihulls and relatively increased roll stiffness..

Full-scale measurements of wave loads and vessel responses are extremely valuable in verification of design predictions. However since sea trials are expensive to conduct, results for high-speed multihulls are very limited in the published literature. Exceptions include the work of Steinmann et al. [2], Roberts et al. [3] and Davis et al. [4].

Thomas et al. [5] reported on full-scale measurements of slam events on large INCAT Tasmania catamarans to investigate slamming behaviour in a variety of sea conditions. The full scale results were then used to determine the influence of the presence of slam events on fatigue life. In addition the effects of significant wave height, slam occurrence rates, slam peak stresses, whipping behaviour on fatigue life were examined. Amin et al. [6] presented a new technique to predict sea loads for high-speed wave piercing catamarans based on finite element modelling and sea trials data. The sea trials data was for a 98 m INCAT Tasmania sea-frame configured to U.S. Navy specification. Wavelet analysis was applied to identify slamming and whipping in full scale records as outlined by Davis et al. [7]. A continuous wavelet transform of a strain gauge time signal reveals details of the response of the vessel to slamming with respect to both frequency and time.

Fu et al. [8] reported on an Office of Naval Research (ONR) sponsored project to obtain full-scale qualitative and quantitative wave slamming and ship motion data on the X-craft, an 80 m high-speed catamaran. During the trials described in the paper, the significant wave height ranged from 1.5 to 2.7 m and the ship speed was between 20 and 40 knots. To provide suitable full-scale validation data, the incoming waves were characterised using a LIDAR system, an array of ultrasonic distance sensors and several video cameras. Three fibre optic gyros were deployed to record ship motions and a GPS unit was used to measure ship speed, pitch, roll, and heading.

This current paper reports on a systematic analysis of high-speed catamaran motions in a seaway. The data obtained in the extensive full scale trials conducted by the U.S. Navy on a 98 m INCAT Tasmania catamaran has been used to assess the vessel's seakeeping performance. Emphasis was placed on the assessment of the ship's response in the frequency domain by calculating its motion RAOs. By characterising the environmental conditions conclusions about the vessel behaviour for different headings, sea states and speeds could be made. Visually observed headings from the full-scale trials were compared to headings calculated from the ship's pitch and roll motion response to the waves. Since the ship was equipped with a ride control system the effect on motion reduction in different conditions could be assessed. In addition RAOs from the full-scale trials were compared to numerical predictions made with *BEAMSEA*, a two dimensional Green function time domain strip theory program developed by Davis and Holloway [9]. This program has the capacity to simulate the effect of the ride control system influence on the vessel motion.

2. FULL-SCALE TRIALS

Systematic full-scale trials were conducted by the U.S. Navy with INCAT Tasmania catamaran hull 61 while operating in coastal waters off Norway and off the north-west coast of the United Kingdom in the North Atlantic [10]. Parts of the collected data were used to systematically analyse the ship's seakeeping performance at different speeds and headings in different sea states. Also the influence of the ride control system on the ship's motion is assessed.

2.1 VESSEL DETAILS

Hull 61 *HSV-2 Swift* is a 98 metre wave-piercer catamaran, designed by Revolution Design and built by INCAT Tasmania. The base vessel was configured to U.S. Navy specifications by adding a flight deck, helicopter hangar and a starboard aft slewing stern ramp to accommodate heavy roll on / roll off vehicles. As seen in Figure 1 it has, like all INCAT Tasmania Wave Piercing high-speed catamarans, a prominent centre bow above the waterline. The aim of this design feature is to reduce pitch motion by providing additional forward buoyancy force when encountering large waves effectively eliminating bow submergence events. Compared to previous INCAT Tasmania vessels the bow clearance was increased to reduce the bow impact load.

Figure 1: Hull 61 *HSV-2 Swift*

Table 1: Hull 61 *HSV-2 Swift* Main Parameters

Length overall	97.22 m
Length waterline	92.00 m
Beam overall	26.6 m
Draft	3.43 m
Demi-hull beam	4.50 m
Deadweight	680 t
Displacement	1670 t
Speed	38 knots (operational) 42 knots (lightship)

The main parameters of the vessel can be seen in Table 1. To increase passenger comfort and range of operability the vessel is equipped with an active ride control system. This includes active trim tabs mounted at the transom and a retractable T-foil with active control elevator tabs, mounted on the centreline plane at the aft end of the centre bow. The ride control system (designed by

NAIAD (Maritime) Dynamics US Inc.) was set up primarily as a pitch damping system with gains adjusted to maximise control effort and benefit in specific sea states.

2.2 MEASUREMENTS

To monitor the seakeeping behaviour the ship was fitted with a series of sensors and signal tie-ins to the ship operating system were made. Ship accelerations, angles and accelerations were measured at different locations. Roll and pitch was measured by mounting a rate sensing gyro at the LCG. To measure accelerations three axis accelerometers were mounted at the bow, bridge, LCG and flight deck using a mounting technique that guaranteed accuracy of frequency response. The instantaneous absolute wave height was recorded using a Tsurumi Seiki Co. Ltd radar based wavemeter mounted on the bow. The accuracy of all these measuring systems was approximately 1%. Accelerations were measured using Columbia sensors (+/-0.01g), rotational measurements using Watson rate gyros (+/-0.025 deg/s) and sea surface position using a TSK radar (+/-1.4cm). However, greater uncertainty in making ship motion measurements is associated with variability of sea conditions, both with respect to direction and whether statistically stationary conditions persisted during a full data record. Data acquisition periods of approximately 30 minutes were adopted on each heading and whilst this is generally accepted as being sufficiently long for the determination of RAOs, it is inevitable that sea conditions are not perfectly unidirectional nor of consistent spectral composition during a 30 minute trial record. Therefore it will always be difficult to assign a reliable accuracy to derived parameters such as RAO values.

To investigate the overall seakeeping performance with respect to the relative heading, octagonal pattern tracks were followed for different vessel speeds and ride control settings. Each octagon consisted of five legs starting with a head sea run and changing the course by 45 degrees until following seas were reached, with the vessel operating at a constant speed and ride control system fully active or partially inactive. The ride control system trim tabs at the stern were always active and the T-foil was either deployed and active or retracted. The length of each leg was varied according to the relative heading to the wave direction. As encounter frequency increases in head seas and reduces in following seas, the recording time in head and bow quartering seas was reduced from 30 to 20 minutes and in stern quartering and following seas was extended to 40 minutes.

2.3 DETERMINATION OF WAVE DIRECTION

During the full-scale trials, the wave direction was determined by visual observation. Results from these observations are always only approximate directions with a low directional resolution, normally being +/-45 degrees. Poor visibility due to the weather conditions or darkness can also reduce the accuracy of visual observations. Due to these problems the method proposed by Davis et al. [1] was used to derive the ship's relative heading from its motions. In this approach the ship is treated in a similar manner to a directional wave rider buoy. The wave direction is determined by the heave (x_{30}), roll (x_{40}) and pitch (x_{50}) motions. Bearing in mind the characteristics of the ship's motion response to the waves, as evident in the RAO functions, it can be seen that for low wave frequencies and thus larger wavelengths, the response amplitude operators approach unity. As a result, the ship's heave represents the surface elevation of the wave and roll and pitch motions describe the wave slope. This approach can be seen as accurate for headings from head to beam seas, since the main ship motions with low frequencies are dominated by responses to larger wave lengths. Due to the forward ship speed nonlinearities in the ship motions for following seas are expected and thus are not likely to be well estimated by this method. The main wave direction is identified as the direction of the maximum angular slope of the ship, caused by pitch and roll motions. Thus, by observing the ship general motion in waves, it can be seen that motions with dominant pitch are due to head seas and dominant roll motions are due to seas coming from the beam direction. Using the pitch and roll motions, the resulting angular slope of the ship can thus be determined. Calculating the motions of the ship deck plane from the roll and pitch vector, measured at the LCG, the dihedral angle between the deck plane and the water surface plane can be calculated using their normal vectors.

$$\sin\left(x_s\right)=\left(\frac{\left|n_s\times n_w\right|}{\left|n_s\right|\left|n_w\right|}\right) \tag{1}$$

$$\sin^2(\mathrm{x_s})=\frac{\tan^2\left(-x_{50}\right)+\tan^2(x_{40})}{\left(1+\tan^2\left(-x_{50}\right)+\tan^2\left(x_{40}\right)\right)^2} \tag{2}$$

The resulting normal vector of the deck plane gives the direction of the inclination angle.

$$\tan\left(x_{6w}\right)=\frac{\tan(x_{40})}{\tan(-x_{50})} \tag{3}$$

Since a certain slope of the deck can be the result of two wave directions that differ by 180 degrees the heave accelerations are used to determine whether the ship is on the front or on the back slope of the wave. By multiplying the magnitude of the calculated slope $|x_s|$ with the heave velocity $\mathrm{d}x_{30}/\mathrm{d}t$, the ship position on the wave can be identified. Where $\mathrm{d}x_{30}/\mathrm{d}t$ is negative, the ship will be on the back slope of the wave, the wave direction being $\mathrm{x_{6w}}$. Thus plotting $|x_s|\ \mathrm{d}x_{30}/\mathrm{d}t$ over x_{6w} gives a range of resulting deck slopes, depending on the wave direction. Considering the heave velocity in this way, there will be two peaks, the negative peak indicating the dominant wave direction.

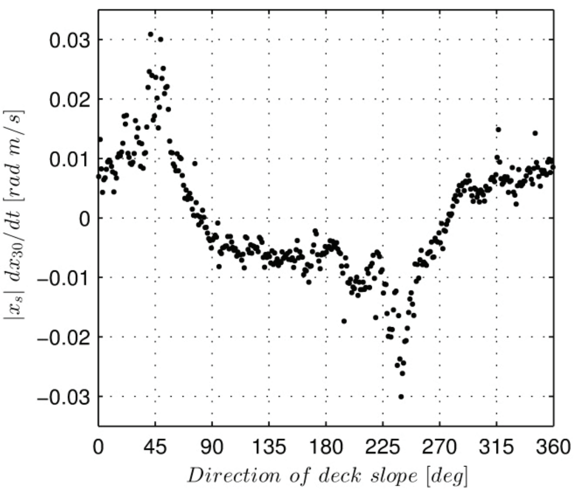

a) Run 160 (bow quartering sea, 1.74m significant wave height, 30 knots, T-foil retracted)

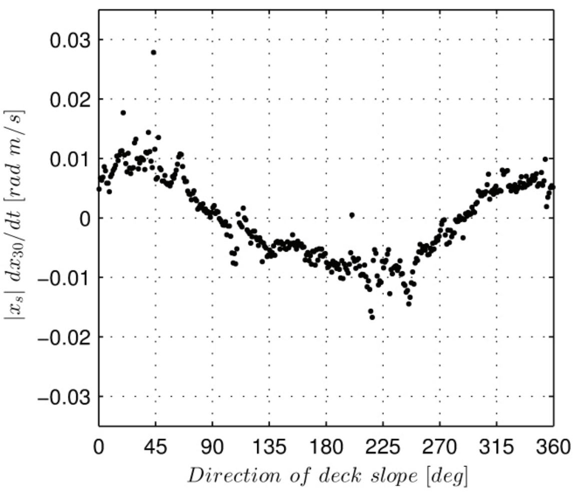

b) Run 153 (bow quartering sea, 1.38m significant wave height, 30 knots, T-foil retracted)

Figure 2: Determination of sea direction from instantaneous ship motions for trial runs 153 & 160

Figures 2 (a) and (b) show examples for a bow quartering sea run. Since the seas were not unidirectional, a distribution of the ship deck slope multiplied by the vertical acceleration between 0 and 360 degrees had to be plotted. As described, the negative peak indicates the ship heading relative to the encountered waves. The positive peak shows the position of the ship on the front of the wave and indicates the opposite wave direction which is 180 deg from the incident wave direction. While Figure 2 (a) shows a good estimation of the ship's heading, the peak values being in a narrow band, Figure 2 (b) shows a weaker peak in response to the waves with the peak values being spread over a rather wide range of heading angles. To identify the actual heading, a range of headings near the maximum and minimum were taken from the plots and the mean values for this range calculated. The deviation of the observed headings about this measured mean was calculated; if the deviation was more than ±22.5 degrees of the observed heading, the run was disregarded. As a result only half of the complete data set was used for later systematic analysis. However, most of the accepted sampled data runs were found to show a direction close to the visually observed direction and over the 37 data runs finally analysed the average deviation between the observed and computed seas direction was only 0.15 degrees of heading with a standard deviation of 10.9 degrees. Only four of these accepted runs had deviations in excess of 12.5 degrees. The cause of the discarded runs having larger deviations would be the difficulty of visually estimating the sea direction and also due to variability of sea direction during the run and with wavelength. In the main larger deviations arose for bow quartering seas, where the sea direction is less easy to estimate than for head and beam sea conditions.

2.4 SPECTRUM AND RAO CALCULATION

To obtain the ship motion RAOs, motion and wave data needed to be converted from time domain to frequency domain using the discrete Fourier transform. The resulting energy density spectra were smoothed using Welch's modified periodogram method [11]. To reduce the variance in the spectrum, the time domain raw data was split into multiple segments and the smoothed spectrum calculated as the average of the segment spectra. To avoid spectral leakage which is due to splitting the data into multiple segments, a window function was applied to every single segment. At a sample rate of 100 Hz a Hanning window with a length of 8000 samples provided good resolution. The overlapping of each window was 50 %, to prevent a loss of information due to the window function.

Response amplitude operators were calculated in encounter frequency domain as the ratio of measured motion energy spectrum to the measured wave energy spectrum. The heave motions x_{30} are related to the wave elevation ζ_0 to give the RAO for heave as

$$\frac{x_{30}}{\zeta_0} = \sqrt{\frac{S_{x3}(\omega_e*)}{S_\zeta(\omega_e*)}}\,, \tag{4}$$

where S_{x3} is the heave motion energy spectrum and S_ζ the wave height energy spectrum. The angular motions in roll x_{40} and pitch x_{50} are normalised by the wave slope to give the RAO values:

$$\frac{x_{40}}{k\zeta_0} = \sqrt{\frac{S_{x4}(\omega_e*)}{S_\alpha(\omega_e*)}}\,, \tag{5}$$

where S_{x4} is the roll motion energy spectrum and S_α the wave slope energy spectrum. All RAOs are presented as a function of dimensionless encounter frequency ($\omega_e^* = \omega_e\sqrt{L/g}$). Since the wave slope cannot be reliably determined for stern quartering and following seas, in this paper only headings from head to beam seas are discussed here.

3. SYSTEMATIC ANALYSIS OF FULL-SCALE DATA

Response amplitude operators gained from the full-scale trials were used to assess the ship's behaviour regarding different sea states, speeds and the influence of the ride control system. Since the trim tabs at the stern were always active, only the effects of the T-foil could be assessed since it was completely retracted for several octagons and fully deployed and active for other octagons. Each analysis was conducted for heading angles from head to bow quartering seas. Within the octagons which were found to be valid in terms of sea direction, appropriate conditions were found to assess the desired RAOs. To analyse the global motion response, RAOs for heave, pitch and roll motions were then plotted for every condition and heading.

3.1 INFLUENCE OF SPEED

To observe the influence of speed on the ship motions, octagons with Froude numbers of 0.25 and 0.5 were chosen for comparison. These correspond to speeds of 15 and 30 knots, allowing the low speed and high speed behaviour to be identified. The significant wave height in both octagons varied between $H_{1/3} = 1.6 - 1.74$ m. This is a rather small range and so the sea conditions can be assumed to be similar. The heave motion RAOs are shown in Figures 3(a) and (b). It can be seen that for all heading angles the heave increases with increasing vessel speed. In these dedicated trials the ship was steered as near to the three heading directions as could be judged visually and so the data is expected to be concentrated in the area of these directions. As has been discussed it was found from the directional analysis that on average the sea direction was very close to the visually observed direction used to steer the ship and that the standard deviation across all data analysed was 10.9 degrees. The dependence of heave motions on the heading angle can be seen as relatively small. The heave in head seas is slightly larger than in beam seas. For the low speed conditions the RAOs are similar and all have a clearly defined peak between ω_e^*=4.7 and 4.8 and amplitudes from 0.7-0.9 times the wave height. At high speeds, the heave motion RAO of the catamaran increases and is in a range from 1.6 up to 1.8 times the wave height. While the head sea run has a well-defined peak at ω_e^*=4.7,bow quartering and beam sea runs have multiple peaks, with the maximum peak being at lower frequencies in the range from ω_e^*=3.9 to 4.1.

The strong heave resonance for *Fr*> 0.5 is similar to that observed in the seakeeping model tests of Wellicome et al. [12], where a peak in heave RAO was found at ω_e^*=4 with an amplitude two times the wave height [13]. Measurements of van Veer et al. predict an even larger heave response of 2.5 times the wave height [14]. The difference can be explained by the hull form: due to the wave-piercing hull and centre bow, a smoother ride is expected for *HSV-2 Swift*.

The pitch response is shown in Figures 3(c) and (d). As would be expected in beam seas the pitch response is small and not affected by speed since the encounter frequency remains the same. Peaks can be identified at ω_e^* = 3.5 and 3.7. In bow quartering seas, the pitch response increases as expected with increasing speeds. We can identify for *Fr*=0.5 peaks at ω_e^* = 3.5 and 4.9. There is a shift along the frequency axis for the high speed run, having peaks at ω_e^* = 3.9 and 5. A similar effect can be seen for the head sea run, but without any increase in the peak value. The low peak value in the head sea run at high speed could be due to the more efficient effect of the trim tabs and T foil at high speed on the pitch motion than on the heave motion. Another reason for the low peak values could be the damping effect of the centre bow on pitch motion in head seas.

As can be seen in Figures 3(e) and (f), the roll motion RAO for both speeds in beam seas is lower than in head seas. However, it should be noted that the range of encounter frequency shown in these results is above that at which maximum rolling is expected. It can be seen that the Roll RAOs are all increasing rapidly as ω_e^* reduces towards 2.0 the lower limit adopted for this analysis. Therefore the trends evident figures 3(e) and (f) are most likely due to the fact that the responses shown are for wavelengths much shorter than that which induces maximum rolling motions. Additionally, the observed trend may be influenced by the ride control system which is acting most strongly to reduce pitch reduction in head seas and may be less effective therefore in controlling roll motions as the system has limited maximum control surface deflections. In this context it is also noted that the observed rolling responses are not large at the frequency of maximum heave and pitch at high speeds and so it is clearly more difficult for the ride control system to be as effective in controlling roll. As has already been noted these results are also significantly affected by the fact that the nominal head seas conditions were not always exactly head seas at 180 degrees to the vessel axis and so even relatively small departures from the exact head sea direction may cause significant rolling. For high speeds, the RAO in head seas has two significant peaks at ω_e^*= 4 and 4.7. The highest roll motion response is observed measured for bow quartering seas this emphasising the influence of wavelength as well as frequency on the rolling motion. Both high and low speed runs have the same peak values with 1.25 times the wave slope, but of course there are larger roll RAOs developing at lower encounter frequencies. As has already been seen for pitch motion RAO, the (small) peak values are shifted along the frequency axis from ω_e^* = 3.1 at *Fr*=0.25 to 3.9 at *Fr*=0.5. However it will be seen in the following section that the variation of the roll RAO is different in larger seas states, reaching the largest values in beam seas.

3.2 INFLUENCE OF WAVEHEIGHT

To investigate the influence of the sea state on the ship motions, octagons with similar speeds but different wave heights were chosen for analysis and interpretation. Since the focus lies on the ship motions at high speeds, octagons with speeds of 30 to 35 knots and wave heights of 1.38 m and 2.01 m were picked. As can be seen in Figures 4(a) and (b) there is a strong heave motion response for all heading angles at both wave heights. For both the low sea state and the high sea state, the heave RAO peak values are similar with values around 1.8 times the wave height. Comparing to Figures 4(a)and (b) it is clear that the heave motion RAO is more sensitive to the speed than to wave height.

The pitch motions are shown in Figures 4(c) and (d), and for both wave heights the expected decrease pitch between head and bow quartering seas can be seen. In head and bow quartering seas, the response for both sea states can be seen as similar although in low sea states there is a more dominant peak. For beam seas there is a clear difference between pitch motions in the two sea states, with a stronger pitch response in high sea states. It appears that in higher sea states there is increased centre bow action in head seas but that in beam seas this effect is reduced.

The roll motion RAOs at the two wave heights can be seen in Figures 4(e) and (f). Compared to heave and pitch motions, we see that the sea state influences the rolling RAO more strongly. For a high sea state, as might be expected intuitively, the roll motion RAO increases from head to beam seas. Whilst there is a clear peak roll RAO at ω_e^* = 4.5 in head seas, the roll motion RAO at other headings increases with decreasing frequency and no peak value was observed here. In low sea states, the roll motion RAO for head and bow quartering seas are higher than in beam seas as discussed in the previous section. In beam seas, the roll motion RAO is substantially lower for lower sea states. As discussed in the previous section it appears that these results come about due to several factors, including the operation of the ride control system, which has a limited range of deflections, as well as the effect of the centre bow, which is stronger in larger seas, and the overall inter relationships between wavelength, sea direction and encounter frequency and ship dynamic response.

3.3 INFLUENCE OF RIDE CONTROL SYSTEM

Since the trim tabs were always active during the runs, only the influence of the T-foil on the ship motions can be evaluated. The T-foil was retracted for several runs and so a comparison of runs with retracted and active T-foil can be made. Being mounted on the centre of the vessel no significant influence on the roll motions is expected. Since the ride control system is much more effective at high speeds when larger vertical forces can be generated, octagons at 30 knots in a wave height range of 1.74 to 1.9 m were chosen for analysis.

In Figures 5(a) and (b) the heave motion response is shown and it can be seen that the T-foil reduces the heave motion RAO significantly for all heading angles. Figures5(c) and (d) show a much smaller influence on pitch motion due to the T-foil. Both octagons show the pitch decreasing from head to bow quartering and beam seas. It is evident from these results that the main benefit of the ride control T foil is to reduce the heave motions by about 20% at the frequency of the maximum RAO function and the effect on pitch is somewhat surprisingly limited.

4. COMPARISON OF NUMERICAL PREDICTIONS AND FULL-SCALE TRIALS

In the final part of this investigation, RAOs from full-scale trials were compared with numerical predictions made by the two-dimensional Green function strip theory code *BEAMSEA*. Since *BEAMSEA* works within the time domain, the trim tab and T-foil motions could be applied in the numerical simulations. The control gains were selected on the basis of the RMS and peak to peak values of the trim tab and T-foil motions recorded during the full-scale testing so that the maximum control deflection without stalling or cavitation could be used. Thus the influence of the ride control system on the motion RAOs can be computed with *BEAMSEA* and *BEAMSEA* simulations conducted with active and retracted T-foil. As in the full-scale tests, the trim tabs at the stern were always active. Thus the effect of both the trim tab motion modelling as well as the T-foil motion modelling could be observed.

4.1 TWO-DIMENSIONAL GREEN FUNCTION TIME-DOMAIN STRIP THEORY

Since traditional frequency domain strip theories are only valid up to Froude numbers of 0.4, a method was developed to predict the motions of high-speed vessels by Holloway and Davis [14]. Using a time domain method was also motivated by the desire to include the effect of ride control systems. The time domain strip theory differs fundamentally from traditional methods in the frequency domain, since they assume the motions to be periodic and a moving reference frame has to be used to simplify the problem. In the time domain this assumption is not necessary and thus a fixed reference frame can be used. Considering the surface boundary conditions, the advantage of a fixed reference frame can be seen as the fluid strips are stationary and fixed in an absolute reference frame. A strip is undisturbed until the bow reaches it and after the ship has completely passed a strip solution for that strip is discontinued behind the ship stern transom. Calculating the problem for each strip in a stationary reference frame using the transient, two dimensional Greens function for a long slender hull satisfies the free surface boundary condition and greatly simplifies the solution. Being dependent on the forward vessel speed in a moving reference frame, the boundary condition can be written as

$$\left(\frac{\delta}{\delta t}-U\frac{\delta}{\delta x}\right)^2\phi+g\frac{\delta\phi}{\delta y}=0 \tag{6}$$

Assuming the ship to move in the +*x* direction with a velocity *U*, no speed dependent terms are required in a fixed frame of reference and the boundary condition simplifies to

$$\frac{\delta^2\phi}{\delta t}+g\frac{\delta\phi}{\delta y}=0 \tag{7}$$

This makes the theory suitable for high speeds with *Fr*> 0.4.

To calculate the hydrodynamic forces on each strip, a panel method is used. Thus any problem can be described by its boundary conditions and no information about the inner flow field is needed. Each panel is described by a source and on the basis of the linearity of Laplace's equation, the potential of each strip can be calculated as the sum over all panels of a source function *f* integrated over all panels.

$$\phi(z,t)=Re\left\{\sum_{j=1}^{n}\int_{panel\ j} f\,ds\right\} \tag{8}$$

For a two dimensional time domain strip theory a Green function given by Wehausen and Laitone [15] is used as the source function.

$$f(z,t)=\frac{Q(t)}{2\pi}\ln\left(z-c(t)\right)-\frac{Q(t)}{2\pi}\ln\left(z-\bar{c}(t)\right)$$
$$-\frac{g}{\pi}\int_0^t Q(\tau)\int_0^\infty\frac{1}{\sqrt{gk}}e^{-ik(z-\bar{c}(\tau))}sin\left[\sqrt{gk}(t-\tau)\right]dk\,d\tau \tag{9}$$

where Q is the source strength, *k* is the wave number, *z* is the complex coordinate of the collocation point, *c* is the source location and $\bar{c}$ its complex conjugate. The first two terms describe the usual double body source, found in free surface problems and the convolution integral generates the required waves. The convolution integral also memorises the flow, to deal with the dynamic boundary problem. The Green function satisfies automatically the linearised free surface boundary condition, and as a result there is no need to consider the free surface at all. Other methods, like the simple source method, require panelling of the free surface which has to be truncated at a certain distance of the ship, since an infinite extended surface cannot be handled in the equations. To get the final pressures on the hull surface

$$p=-\rho\frac{\delta\phi}{\delta t} \tag{10}$$

has to be determined. Calculating ϕ with the help of (3.33) and (3.34) and differentiating the potential gives

$$\frac{\delta\phi_{i,j}}{\delta t}=Re\frac{e^{-i\beta}}{2\pi}\left[\left(A_k+\left(z-c_k\right)B\right)\ln\left(e^{-i\gamma}\left(z-c_k\right)\right)\right]_{k=1}^2$$
$$-\frac{e^{i\beta}}{2\pi}\left[\left(\bar{A}_k+\left(z-\bar{c}_k\right)\bar{B}\right)\ln\left(z-\bar{c}_k\right)\right]_{k=1}^2$$
$$+\frac{2ig}{\sqrt{\pi}}\int_0^t e^{i\beta(\tau)}Q(\tau)\int_{w_1}^{w_2}\left(e^{w^2}\mathrm{erf}w+\frac{1}{w\sqrt{\pi}}\right)dw\,d\tau \tag{11}$$

where $w=\frac{i(t-\tau)}{2}\sqrt{\frac{-ig}{z-\bar{c}(\tau)}}$, $\bar{A}_k=Q\frac{dc_k(t)}{dt}$ and $B=-\frac{dQ}{dt}+iQ\frac{d\beta}{dt}$. To solve this set of equations, the source strengths Q_i have to be obtained. This can be done meeting the boundary conditions on the hull. Recalling that the ship is observed in a non-moving reference frame, the boundary conditions on the hull can be written as $\nabla\phi\hat{n}=\vec{V}\vec{n}$, that is that the fluid velocity and body velocity are compatible and velocities in the normal direction to the hull surface are equal. By using a non-moving reference frame, the local hull element velocity can described by $\vec{v}_{\mathrm{hull}}-\vec{v}_{\mathrm{wave}}$.There is no distinction made here between radiated and diffracted waves. Since the Green function automatically satisfies the free surface condition, the latter is not considered. Using the complex velocity

$$W=\frac{\delta(\phi+i\psi)}{dz}=u-iv \tag{12}$$

and using equation (3.33), the velocity for each collocation point *i* at *z* can be described by the source strength on each panel *j*.

$$W_{i,j}=\frac{Q}{2\pi}\left(e^{-i\beta}ln\left(\frac{z-c_1}{z-c_2}\right)-e^{-i\beta}ln\left(\frac{z-\bar{c}_1}{z-\bar{c}_2}\right)\right)$$
$$-i\sqrt{\frac{g}{\pi}}\int_0^t e^{i\beta(\tau)}Q(\tau)\left[\frac{e^{w^2}\mathrm{erf}w}{\sqrt{i\left(z-\bar{c}\right)}}\right]_{w_1}^{w_2}d\tau \tag{13}$$

with the slope of each source element being β = arg (c_2 - c_1). Since the convolution term contains only the already known previous source strength terms, it can be separated from the first part of the equation. With the help of the boundary condition at the hull, the unknown source strengths for the current time step can be described in matrix form

$$[A]\{Q\}=\{R\} \tag{14}$$

With $A_{i,j}$ describing the influence of the ith boundary condition equation due to the source Q_i, and R_i representing the term in the boundary conditions independent of Q. Concerning (3.37) both can be written as

$$A_{i,j}=-Im\left\{\frac{e^{i\alpha}}{2\pi}\left[e^{-i\beta}ln\left(\frac{z-c_1}{z-c_2}\right)-e^{-i\beta}\ln\left(\frac{z-\bar{c}_1}{z-\bar{c}_2}\right)\right]\right\} \tag{15}$$

$$R_i=\vec{V}\hat{n}-Im\left\{e^{-i\alpha}\left[\sqrt{\frac{g}{\pi}}\int_0^t e^{i\beta(\tau)}Q(\tau)\left[\frac{e^{w^2}\mathrm{erf}w}{\sqrt{i(z-\bar{c})}}\right]_{w_1}^{w_2}d\tau\right]\right\} \tag{16}$$

The convolution integral has to be evaluated numerically, this forming the most computationally intensive part of the solution method.

4.2 NUMERICAL RESULTS

Figures 6(a) and (b) show a comparison of the calculated and measured heave motion RAOs at 30 knots with active and retracted T-foil. The ride control system was modelled as a pitch damper with gains set to give maximum control deflections in a 3 m sea thereby simulating the full scale ride control system. The computed RAOs demonstrate generally good correlation with the full scale results, especially in terms of RAO magnitude. The numerical heave RAOs do however show a discrepancy in the frequency of the peak value when compared with the full scale results, for both cases with the T-foil retracted and active. This shift may be due to an underestimate of the vessel's added mass, especially in the demi-hull region where there is a hard chine which could generate shed vortices not represented in the potential solution.

The numerical *BEAMSEA* results also show that the active T-foil has a significant influence in reducing the heave motion. Also, the effect of the introducing the centre bow is included in the numerical solutions and it can be seen that there is a significant reduction in heave RAO due to the centre bow's influence on the motion damping. The numerical pitch motion RAOs shown in figures 6(c) and (d) correlate very well with the full scale results, both with the T-foil deployed and retracted. There is less influence of incorporating the centre bow into the numerical solution for the pitch results.

5. CONCLUSIONS

A systematic analysis of data recorded during full-scale trials with INCAT Tasmania hull 61 in severe conditions was undertaken. Its seakeeping behaviour and motion response have been determined. Measured motion RAOs were calculated and used to validate the seakeeping code *BEAMSEA* including ride control system effects. Calculation of the motion RAOs for different conditions has shown that Welch's periodogram method is a valid method to estimate wave and motion spectra in this type of sea trial. At a sample rate of 100 Hz a Hanning-window with a length around 8000 samples provided good resolution. The RAOs were calculated for a range of conditions, enabling the ship's seakeeping performance for different headings, speeds and sea states to be assessed. Also the performance of the ride control system was assessed. It was found that a visual observation of the wave direction during full-scale trials is sometimes imprecise due to the difficulty in making precise observations and the complexity of the seas. Therefore a determination of the heading angle using the ship's pitch and roll motion was found to be a good method to verify the visual observations.

The RAOs showed an increase of the heave and roll motion with increasing speed. For the pitch motions there was less evidence of an increase of the peak response with speed. This suggests that there is increasing effectiveness of the trim tabs as pitch dampers at high speeds since it is known that the ride control algorithm employed on these vessels is set up primarily as a pitch damper. With regard to the ship heading, a decrease of pitch and (to a lesser extent) heave RAOs was found in beam seas compared to the motions in head seas. Unexpectedly the biggest peak roll motion RAOs were found in bow quartering seas. This appears to have arisen in part because the RAOs were not determined at the relatively low frequency of maximum rolling, and also owing to limitations of the ride control system in controlling roll when set up as a pitch damper. Further, it was evident that nominally head sea trials were not always in conditions of exact head seas, despite the best efforts of the trials crew to achieve that condition. It is clear that there is a need to further investigate what is the best the ride control system algorithm.

While heave and pitch motion RAOs changed their characteristics with increasing speed, their RAOs are similar for different sea states. For the pitch motion it appears that the pitch damping provided by the centre bow increases in high seas. This explains the higher peak value in the lower sea state beam sea runs in head and bow quartering seas where the influence of the centre bow is diminished. In high sea states it was found that the trim tabs cannot cope as well with large roll motions and in beam seas the high sea state run showed a much stronger roll motion response.

The T-foil was found to significantly reduce the heave motions at 30 knots. However it was found that there was less effect of the T-foil in reducing the pitch motions. This indicates that the stern tabs are perhaps the main contributor to reduction of pitch motion at 30 knots and above. Since the T-foil is mounted at the aft end of the centre bow the centre bow, it would not have maximum possible effect on pitch due to the reduced distance to the centre of mass of the ship and the roll motion was not influenced by the T-foil.

The measured RAOs were also used to validate the seakeeping code *BEAMSEA* and its modelling of the ride-control system. It was shown that using the RMS values of the measured trim tab and T-foil motions to establish appropriate system gains lead to a good prediction of the motion amplitudes. However, while changes in response for the different operating conditions investigated were well modelled, a small discrepancy in the frequency of the peak heave motion to the full-scale trials results was found.

6. ACKNOWLEDGMENTS

The authors acknowledge the work of Naval Surface Warfare Center, Carderock Division, USA in conducting the full scale measurements and thank them for making the data available for analysis.

7. REFERENCES

1. Davis,M.R., Watson, N.L and Holloway. D.S., 2005, Measurements of response amplitude operators for an 86 m high-speed catamaran, Journal of Ship Research, 49 (2) pages 121–143

2. Steinmann, P.,Fach, K. and Menon, B.,Global and slamming sea loads acting on an 86m high speed catamaran ferry. In Proceedings Fast'99, 5th International Conference on Fast Sea Transportation, Seattle, pages 709-718, 1999.

3. Roberts, T.J., Watson, N.L., Davis, M.R., Evaluation of sea loads in high speed catamarans. In Proceedings FAST'97, 4th International Conference on Fast Sea Transportation, Sydney, pages 311-316, 1997.

4. Davis, M.R., Watson, N.L. and Holloway, D.S., Wave Response of an 86m High Speed Catamaran with Active T-Foils And Stern Tabs, The Transactions of The Royal Institution of Naval Architects, Part A International Journal of Maritime Engineering, 145 (A2) pp. 15-34. 2003.

5. Thomas, G., Davis, M., Holloway, D., Watson, N. and Roberts, T.,Slamming Response of a Large High-Speed Wave-Piercer Catamaran,SNAME Marine Technology Journal, Vol. 40, Number 2, pages 126-140, April 2003.

6. Amin, W., Davis, M., Thomas, G. and Holloway, D., Slamming Quasi-Static Analysis of an Incat 98-m High-Speed Wave Piercing Catamaran, In Proceedings International Conference for Innovation in High Speed Marine Vehicles, Fremantle, Australia, 2009.

7. Davis, M.R., Thomas, G., Holloway, D.S., Lavroff, J., Amin, W., Matsubara, S. and Roberts, T.R., Slamming and Whipping of Wave-Piercing Catamarans, Proceedings, In Proceedings Hydroelasticity in Marine Technology, Southampton, UK, 2009.

8. Fu, T.C., Fullerton, A.M., Terrill, E., Faller, W., Lada, G., Hess, D. and Minnick, L., Measurement and modeling of the motions of a high-speed catamaran in waves. In Proceedings 28th International Conference on Ocean, Offshore and Arctic Engineering OMAE2009, Honolulu, Hawaii, USA, June 2009.

9. Holloway,D.S., A High Froude Number Time Domain Strip Theory Applied to the Seakeeping of Semi-SWATHs, PhD thesis, University of Tasmania, November 1998.

10. Brady,T.F., Bachman, R.J., Donnelly, M.J. and Griggs, D.B.,HSV-2 Swift instrumentation andtechnical trials plan. Technical Report, Naval Surface Warfare Center Carderock Division,July 2004.

11. Welch, P.D., T he Use of Fast Fourier Transform for the Estimation of Power Spectra: A Method Based on Time Averaging Over Short, Modified Periodograms, IEEE Transactions on Audio Electroacoustics, AU-15, 70–73, 1967.

12. Wellicome,J.F., Temarel,P.A., Molland,F., Cic, J. and Taunton, D.J., Experimental measurements of seakeeping characteristics of fast displacement catamarans in oblique waves, Ship Science Report 111, Technical Report, Department of Ship Science, University of Southampton, 1999.

13. Van't Veer, A.P., Behaviour of Catamarans in Waves. PhD thesis, Delft University of Technology, September 1998.

14. Holloway, D. and Davis M., Ship Motion Computations Using a High Froude Number Time Domain Strip Theory, Journal of Ship Research, Vol. 50, No. 1,pp15-30, 2006.

15. Wehausen, J.V. and Laitone E.V. , Surface waves, *in* Handbuch der Physik (ed. S. Flügge), v9, pp.445–814, Springer, 1960.

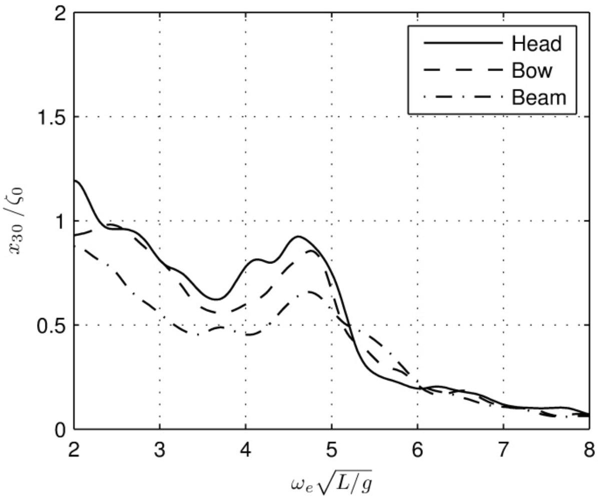

a) Heave RAO at Fr = 0.25

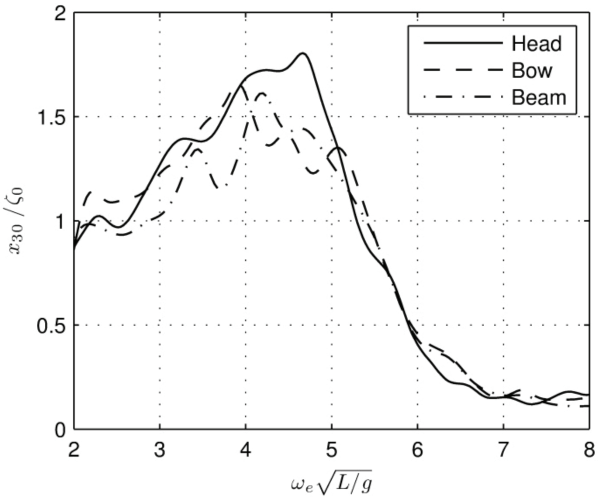

b) Heave RAO at Fr = 0.5

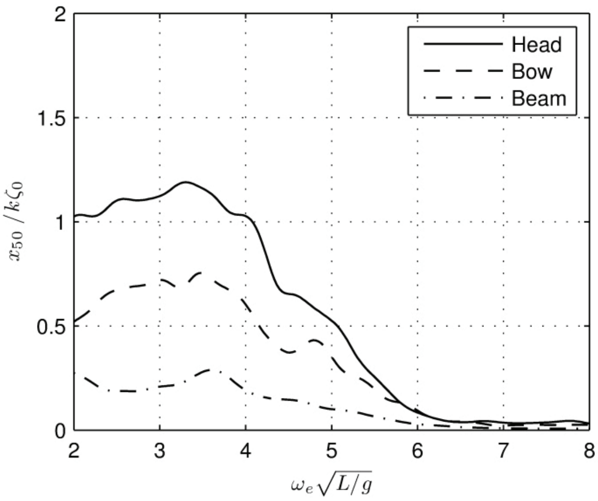

c) Pitch RAO at Fr = 0.25

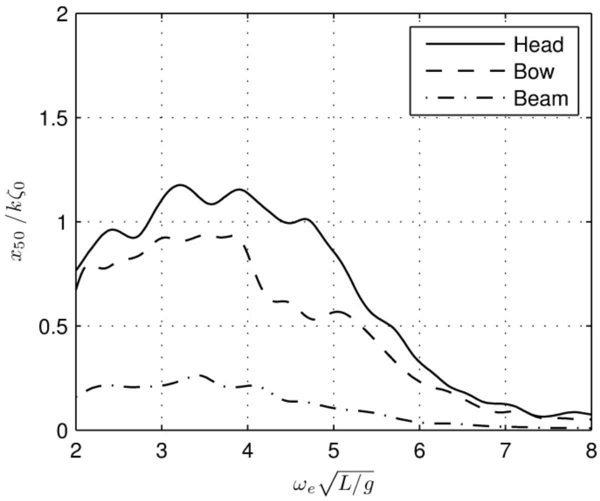

d) Pitch RAO at Fr = 0.5

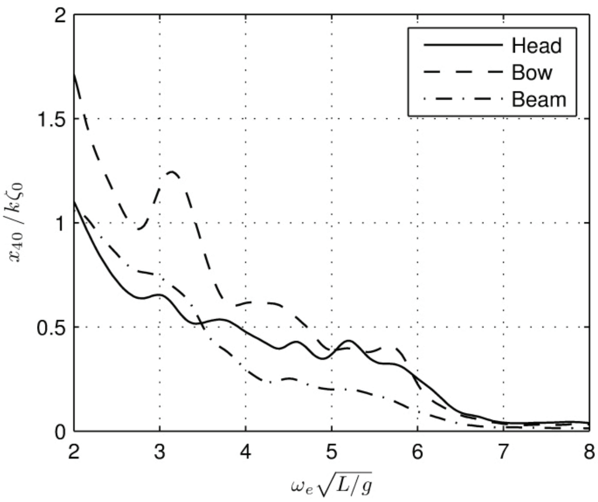

e) Roll RAO at Fr = 0.25

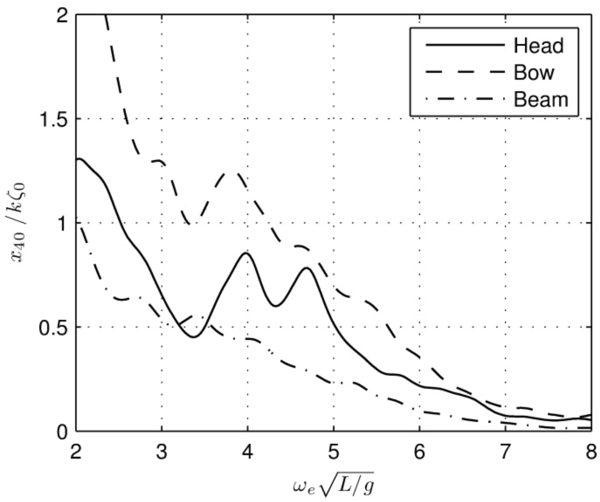

f) Roll RAO at Fr = 0.5

Figure 3: Influence of speed on motion RAOs at $H_{1/3}$ = 1.6 – 1.74 mwith T-foil deployed

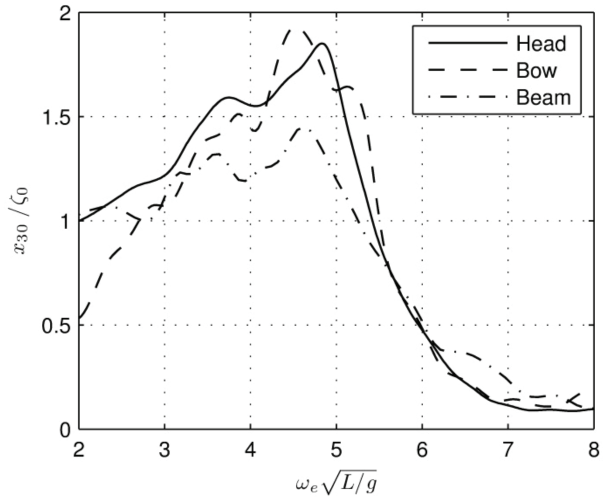

a) Heave RAO at $H_{1/3}$=1.38 m

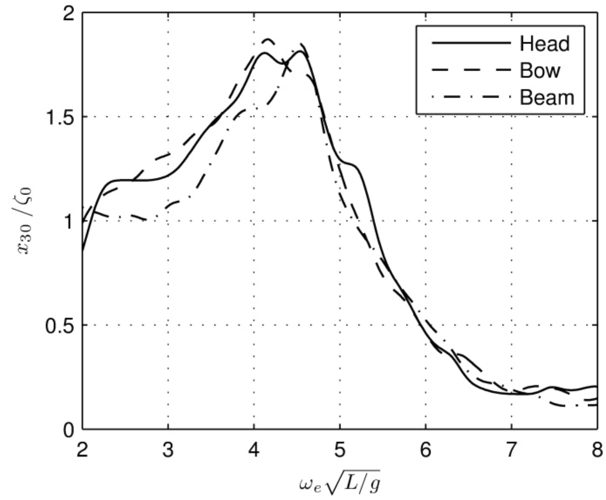

b) Heave RAO at $H_{1/3}$ = 2.01 m

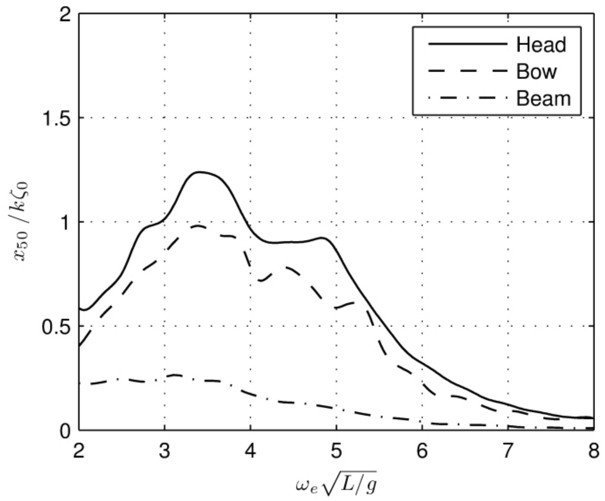

c) Pitch RAO at $H_{1/3}$ = 1.38 m

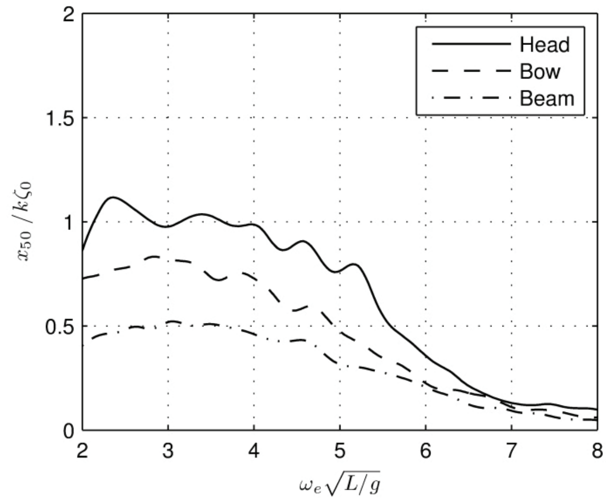

d) Pitch RAO at $H_{1/3}$ = 2.01 m

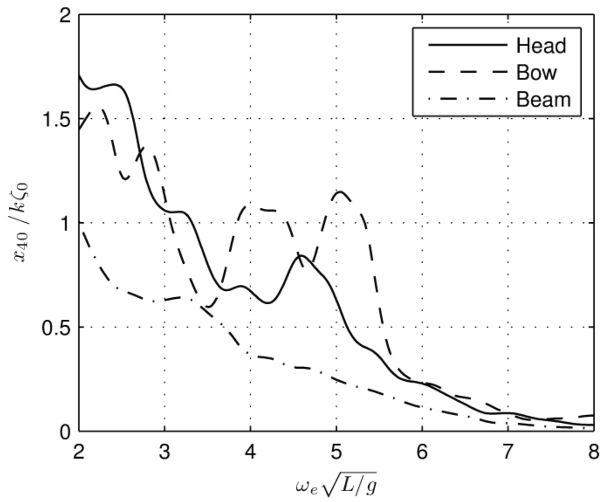

e) Roll RAO at $H_{1/3}$ = 1.38 m

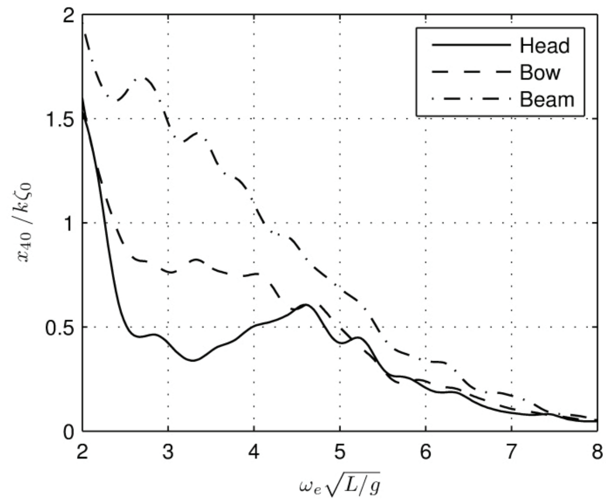

f) Roll RAO at $H_{1/3}$ =2.01 m

Figure 4: Influence of significant waveheighton motion RAOs at 30 - 35 knots with T-foil deployed

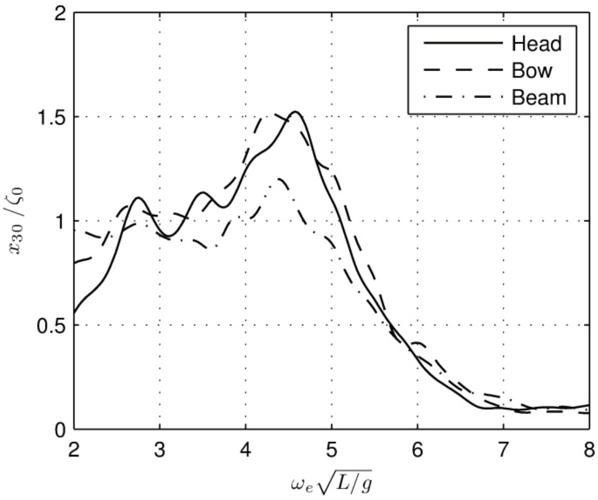

a) Heave RAO with T-foil deployed

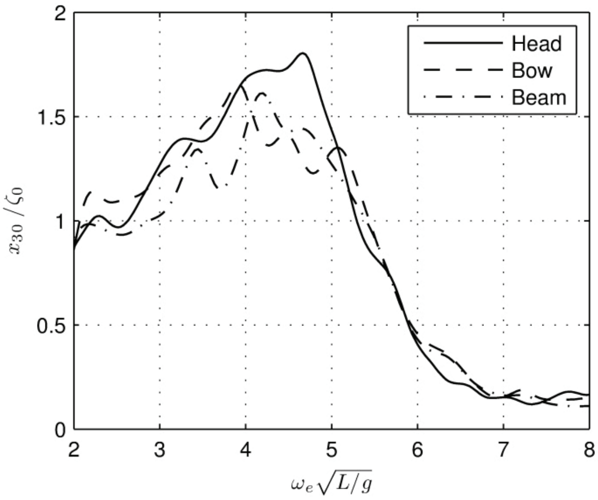

b) Heave RAO with T-foil retracted

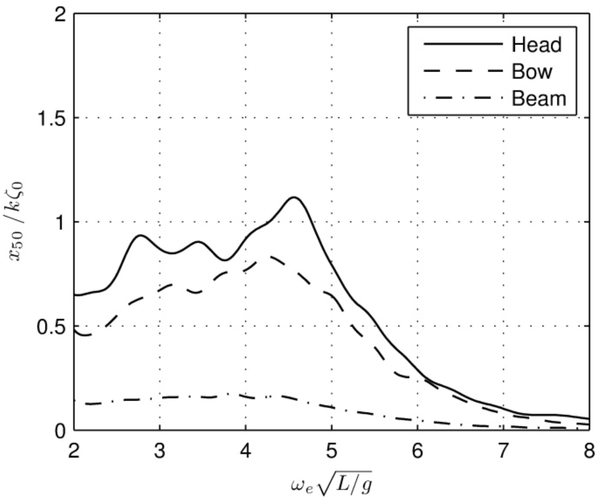

c) Pitch RAO with T-foil deployed

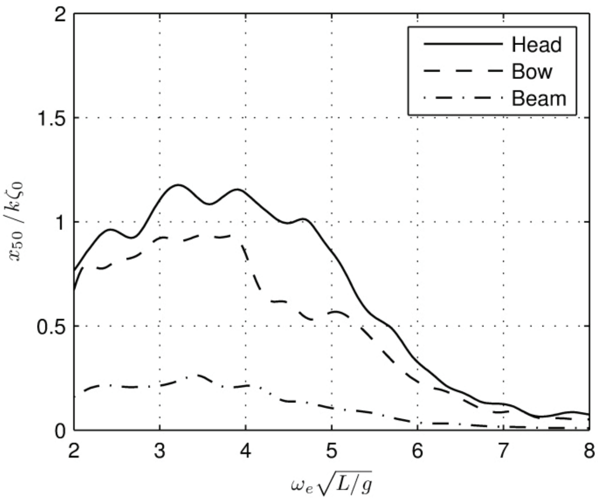

d) Pitch RAO with T-foil retracted

Figure 5: Influence of ride control system on motion RAOs at 30 knots

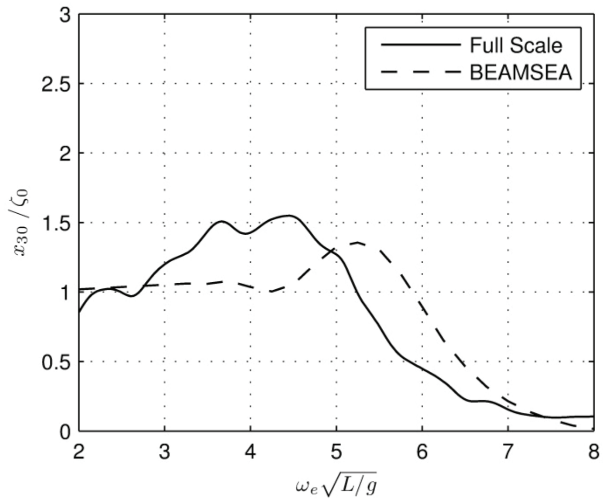

a) Heave motion RAO with T-foil deployed

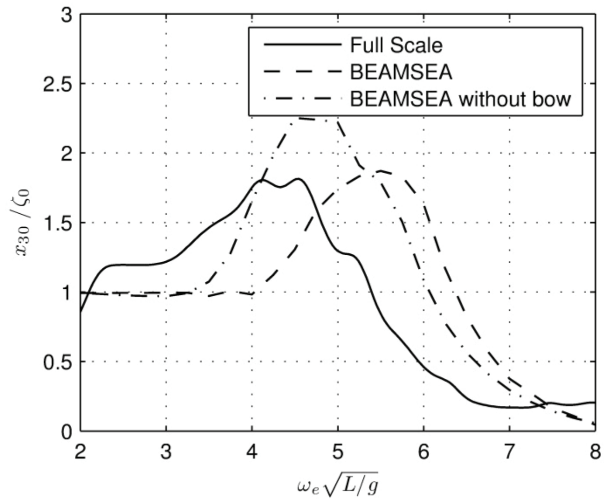

b) Heave motion RAO with T-foil retracted

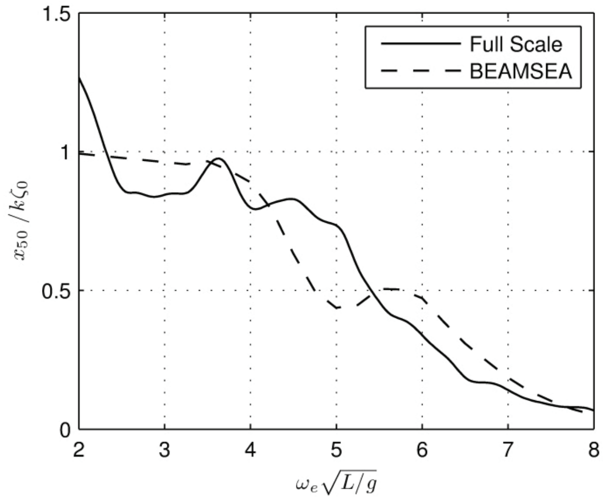

c) Pitch motion RAO with T-foil deployed

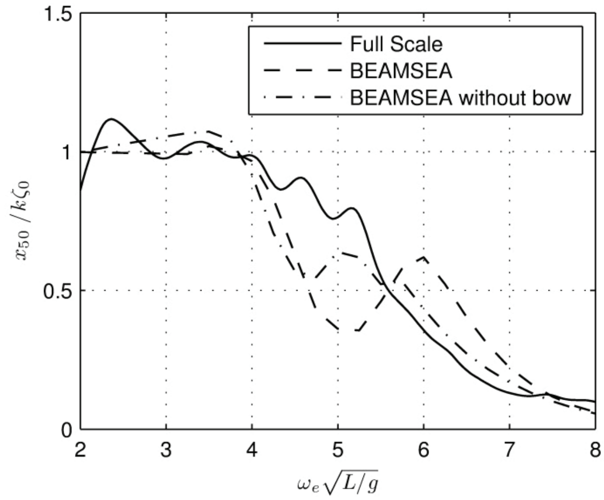

d) Pitch motion RAO with T-foil retracted

Figure 6: Comparison of full-scale and BEAMSEA RAOs in head seas